Polyvinyl alcohol/Polyvinylpyrrolidone/Chitosan Nanofiber Scaffold with Hydroxyapatite from Sand Lobster Shells (*Panulirus homarus*) for Bone Tissue Engineering

I Kadek Hariscandra Dinatha[1], *Arian H.* Diputra[1], *Hevi* Wihadmadyatami[2], *Juliasih* Partini[1], and *Yusril* Yusuf[1*]

[1]Departement of Physics, Faculty of Mathematics and Natural Science, Universitas Gadjah Mada, Yogyakarta, Indonesia
[2]Department of Anatomy, Faculty of Veterinary Medicine, Universitas Gadjah Mada, Yogyakarta, Indonesia

Abstract. In this work, nanofiber scaffold membrane polyvinyl alcohol (PVA)/polyvinylpyrrolidone (PVP)/Chitosan (CS)/hydroxyapatite (HAp) from sand lobster (SL; *Panulirus homarus*) shells have successfully synthesized to mimic the extracellular matrix (ECM) nanoscale in the native bone. HAp was synthesized by co-precipitation method with Ca/P was 1.67, then nanofiber membrane PVA/PVP/CS/HAp was synthesized by electrospinning method. Nanofiber solution was prepared from PVA 10% (w/v) polymer solution that dissolved in the distilled water, then the PVP/CS 15% (w/v) polymer solution was dissolved in acetic acid 1% (v/v) separately. The PVA polymer solution and PVP/CS solution were mixed with a ratio of 8.5: 1.5 (v/v). HAp dispersed into mixture solution with variation concentration 0, 1, 3, and 5 wt%. The composite solution was put into a 10 ml syringe with a hole diameter = 0.5 mm. Electrospinning was carried out at a 10 kV voltage, the flow rate at 0.1 ml/h, and the distance between the collector to the tip was 12 cm. Nanofiber scaffold membrane was characterized using SEM, FTIR, and XRD. The addition of HAp into the fiber showed incorporation into nanofiber with small agglomeration in the concentration of HAp at 1, 3, and 5 wt%. Based on the physicochemical analysis, the nanofiber scaffold PVA/PVP/CS/HAp 5 wt% with a fiber diameter of 0.328 ± 0.049 μm has the most potential to be used for bone tissue engineering.

1 Introduction

Bone is the hard tissue that forms the skeleton of the human body as a support for passive movement [1]. Like any tissue, bones can also be damaged due to injury, traffic accidents, fracture nonunion, bone tumor resection, or degenerative diseases such as osteoporosis [2,3]. Although bone has a particular healing and regeneration capacity, it cannot be accomplished

* Corresponding author: yusril@ugm.ac.id

© The Authors, published by EDP Sciences. This is an open access article distributed under the terms of the Creative Commons Attribution License 4.0 (https://creativecommons.org/licenses/by/4.0/).

by itself for large segmental bone defects [2]. Healing of segmental bone defects remains a challenge because of the limited availability of bone material to fill the defect and promote bone growth [4]. Various studies attempt to make materials to mimic bone structures and have biocompatible, bioactive, biodegradable, and osteoconductive properties to bone tissue. The use of material scaffolds from bioceramic and polymer components to support bone cell and tissue growth is a longstanding area of interest [3]. Therefore, the major challenge in bone tissue engineering is to design and fabricate a suitable scaffold to support bone growth.

The bone at the nanoscale forms an extracellular matrix (ECM) that consist of organic minerals (type I collagen) and is reinforced by inorganic minerals (hydroxyapatite (HAp)) [5,6,7]. HAp ($Ca_{10}(PO_4)_6(OH)_2$) is one part of calcium phosphate, which is the main mineral constituent of human bone and teeth [8,9,10]. About 60-70% of inorganic mineral content in human bone is HAp [11], so bioceramic HAp has biocompatible, bioactive, and osteoconductive properties to bone tissue [12]. HAp has a monoclinic and hexagonal crystal structure. The monoclinic structure has lattice parameters of a = 9.421 Å, b=2a and c = 6.881 Å, while a = b = 9,432 Å dan c = 6,881 Å for hexagonal structure with a molar ratio Ca/P was 1.67 [13,14]. HAp was synthesized by co-precipitation method and derived from sand lobster (SL; *Panulirus homarus*) shells which the lobster molting waste periodically. Incorporating HAp in nanofiber membranes are expected to enhance the scaffold bioactivity.

The ECM structure at the nanoscale in the natural bone forms nanofiber structures. The nanofiber scaffold membrane is one of bone tissue engineering to mimic the ECM structure at the nanoscale in the bone [7]. Nanofiber scaffold engineering will create an environment for the cells similar to the host to stimulate the osteoblast cells to bone growth. Various processing techniques (e.g., phase separation, self-assembly, and electrospinning) have been developed to fabricate nanofiber membrane scaffolds for ECM substitutes [15]. Among them, the electrospinning method has advantages. It can process various materials (organic polymers, colloidal particles, and composites) [16], has cost-effectiveness, and can generate fiber similar to the fibrous structures of native ECM.

In the present study, the polymer solution used as a matrix nanofiber membrane is polyvinyl alcohol (PVA)/polyvinylpyrrolidone (PVP)/chitosan (CS). PVA is an environmentally friendly polymer with advantages such as water solubility, biodegradability, biocompatibility, chemical stability, processability, and excellent spinnability [17]. PVP is a surfactant polymer because of its advantages, such as being soluble in water and acid, non-toxic and stable. PVP has been applied in fields such as pharmacy and biomedical [18]. Although nanofiber scaffold membranes should have non-toxic properties, they should also have antibacterial activity. The CS is a biopolymer derived from the exoskeletons of crustaceans, crabs, and shrimp shells [19]. In addition to the fact that CS was expected to give antibacterial activity to the nanofiber scaffold, CS also has a similar structure to the ECM glycosaminoglycans (GAGs) in the bone [20]. However, the CS has drawbacks, such as low solubility. PVP makes the higher-level solubility of CS so that CS is easier to dissolve. HAp incorporated into nanofiber with concentration varied at 0, 1, 3, and 5 wt%. The nanofiber scaffold membrane was characterized using SEM, XRD, and FTIR to identify their physicochemical properties. Nanofiber PVA/PVP/CS/HAp have the potential to be applied in bone tissue engineering.

2 Material and Method

2.1 Materials

In this study, HAp used calcium ($Ca(OH)_2$) from SL shells (*Panulirus homarus*) as a source of calcium from Buleleng, Bali, Indonesia, and $(NH_4)_2HPO$ (Merck, USA) as a source of

phosphate. NH_4OH 25% 3M (Merck, USA) solution for pH control. PVA (100% hydrolyzed) was purchased from Merck (Germany) with a molecular weight of 145.000, CS medium molecular weight, and PVP with a molecular weight of 10.000 was purchased from Sigma-Aldrich (USA). Acetic acid (100%) was purchased from Merck (Germany).

2.2 Synthesis of HAp

The previous study described the synthesized process of HAp from SL shells[21]. SL shells were cleaned, milled, and calcinated at 1000 ºC for 6 h to obtain $Ca(OH)_2$ powder. A total of 6M $(NH_4)_2HPO$ solution was titrated at a 1 mL/min rate to 10M $Ca(OH)_2$ solution. The pH was controlled at pH 10 by adding NH_4OH 25% 3M. Then the mixture was stirred constantly at 60 ºC to obtain a homogeneous solution. The chemical reaction is shown in Eq. 1 [21].

$$10Ca(OH)_2 + 6(NH_4)_2HPO_4 \rightarrow Ca_{10}(PO_4)_6(OH)_2 + 12NH_4OH + 6H_2O \quad (1)$$

The solution was aged for 24 h at room temperature and continued with the filtering process. The mixture was dried using an oven at 100 ºC for 6 hours and the sintering process at 1000 ºC for 6 hours. Then HAp was characterized using FTIR, XRD, and SEM-EDX..

2.3 Preparation of Electrospinning Solution

PVA was dissolved in the distilled water at a concentration of 10% (w/v). A total of 1.4 gram PVP and 0.1 gram CS were dissolved in the 10 ml acetic acid 1% (v/v), which obtained 15% (w/v) PVP/CS solution. PVA 10% (w/v) solution, then mixed with PVP/CS 15% (w/v) solution, with a ratio of 8.5: 1.5 (v/v). The mixture was stirred until the homogeneous solution was obtained, then HAp was added to the mixture with concentrations of 0, 1, 3, and 5 wt%, then continued stirring until the mixture was homogeneous. Then the solution was used for the electrospinning process.

2.4 Synthesis of Nanofiber Membrane

The solution prepared was put into a syringe of 10 ml with a hole diameter of 0.5 mm. The voltage was applied of 10 kV between the tip to the collector covered by aluminum foil with a distance of 12 cm. The flow rate is automatically at 0.1 ml/h. The solution was maintained at room temperature. The fiber will be formed at the collector as a nanofiber scaffold membrane PVA/PVP/CS/HAp 0, 1, 3, and 5 wt%. It will be characterized by using SEM, XRD, and FTIR.Equations and mathematics

3 Result and Discussion

3.1 Hydroxyapatite (HAp) Powder

HAp synthesized derived from SL shells was characterized to identify their physicochemical properties. The FTIR spectrum results shown in Fig. 1(a) revealed that the mode of PO_4^{3-} stretching was at 946.54 and 1112 cm^{-1}, and the peak of PO_4^{3-} bending mode was at 1019.1 cm^{-1} sharply. The small peak at 1420.65 cm^{-1} indicated the CO_3^{2-} vibration was reduced when given at a high temperature, while the OH^- group appeared at a wave number of 3643 cm^{-1}.

XRD pattern of HAp was confirmed by standard diffraction pattern from JCPDS 09-0432, which formed the characteristics diffraction peak of HAp at angles of 31.18º, 31.72º, 32.85º [22,23] with diffraction planes of (211), (112), and (300), as well as other peaks observed in

Fig. 1(b). The XRD results also showed a β-Tricalcium phosphate (β-TCP) peak in addition to HAp. The β-TCP is a tertiary calcium phosphate with high biocompatibility that can promote improvement in bone tissue [24,25]. The crystal structure analysis of HAp is shown in Table 1. The HAp crystallite size formed was 31.620 ± 4.140 nm with lattice parameters at a = 9.411 Å and c = 6.833 Å. These results were similar to the HAp hexagonal structure and indicated that the dominantly formed crystal phase was HAp[13].

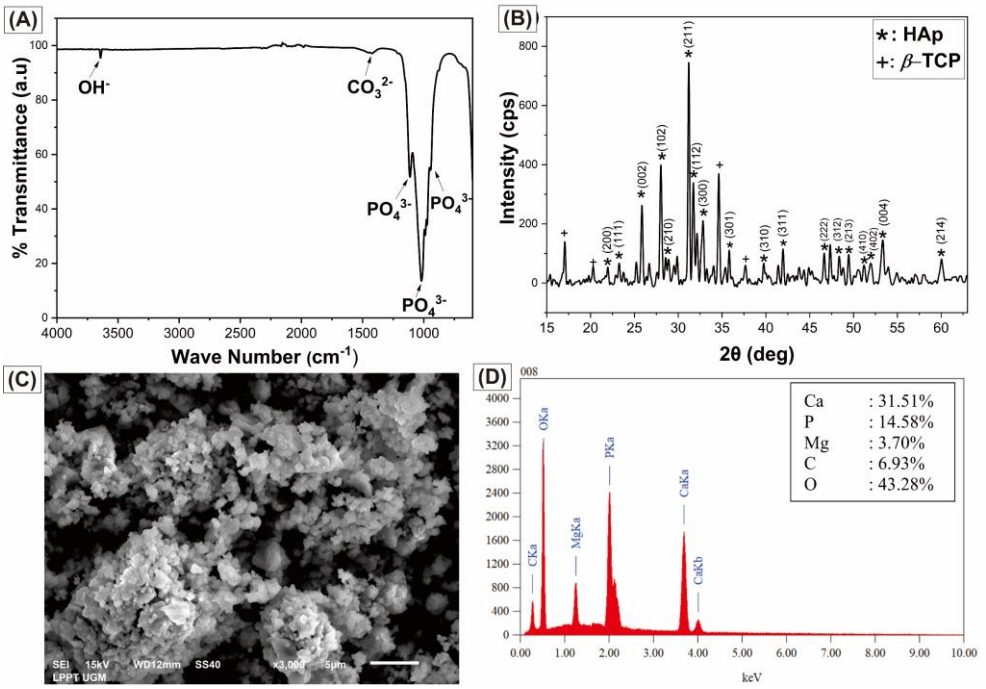

Figure 1. Characteristic of HAp basen on (a) XRD, (b) FTIR, (c) SEM and (d) EDX results

Table 1. Lattice parameter, crystallite size, and microstrain of HAp [21].

Sample	Lattice parameter (Å)		Ratio of *c/a*	Crystallite size (nm)	Microstrain
	a	*C*			
HAp	9.411	6.833	0.726	31.620 ± 4.140	0.021 ± 0.013

The HAp powder has a regular and homogeneous morphology, as shown in Fig. 1(c), with relatively negligible agglomerations. Based EDX analysis (Fig. 1(d)) revealed a Ca mass of 31.51% and a P mass of 14.58%, so the molar ratio of Ca/P was 1.67. This result is suitable with Ca/P in HAp human bone, which is 1.67 [9]. The small impurities of Mg can be neglected because Mg is one of the inorganic minerals of native bone in small quantities [13].

3.2 Scaffold Nanofiber Membrane

Synthesized nanofiber was characterized to identify their physicochemical properties using XRD, FTIR, and SEM. The XRD results are shown in Fig.2(a). The peak of 19.36° corresponds to the PVA/PVP/CS [17,20,26]. The PVA/PVP/CS peak decreased its crystallinity at a higher concentration of HAp. The presence of HAp on the nanofiber could

disrupt the macromolecular chains of the polymer, leading to a decrease in the amount of crystalline polymer. In addition, the interaction between the HAp and the polymer at their interface can also cause the formation of an amorphous polymer layer [13]. The peak showed characteristics of HAp crystal at 25.92[23], 31.81[22], 32.92[23], and 34.68°, which got sharper proportional to the concentration of HAp. These confirm the presence of HAp in the nanofiber membrane. HAp crystal was expected to enhance good biocompatibility, bioactivity, and osteoconductivity at nanofiber to stimulate the cell osteoblast for bone growth.

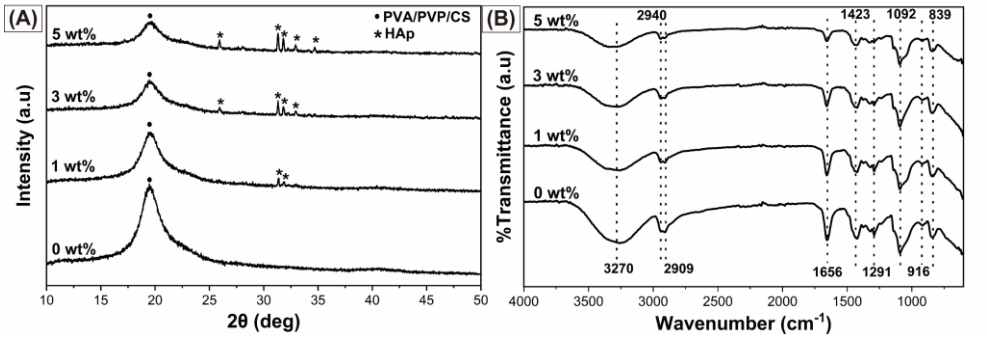

Figure 2. Characteristic (a) XRD, and (b) FTIR of Nanofiber PVA/PVP/CS/HAp with concentration of HAp 0, 1, 3 and 5 wt%

The FTIR results of nanofiber PVA/PVP/CS/HAp are shown in Fig. 2(b). The broad peak at 3270 cm^{-1} is attributed to the hydrogen bonding OH^- group and are overlapped with the stretching vibration of N-H [27]. A shift in the absorption peak occurred at a higher concentration of HAp towards a wave number of 3338 cm^{-1}. These results show that the hydrogen bonding became stronger from HAp [20]. The peak at 2940 and 2909 cm^{-1} are related to the C-H symmetric and antisymmetric stretching vibration, respectively [17,20,28]. The peak at 1656 cm^{-1} indicates the C=O stretching vibration of amide-type I from CS [17]. CH-OH bending was shown at a wave number of 1423 cm^{-1} [28]. The small peak at 1291 dan 916 cm^{-1} corresponds to the C-N stretching of the pyrrolidone ring in the PVP [27], while the sharp peak at 1092 and a small peak at 840 cm^{-1} shows C-O stretching vibration supporting the PVA configuration and C-C bonds [20,28], respectively.

HAp synthesized and then incorporated into PVA/PVP/CS nanofiber membrane as a filler to mimic the structure of ECM in the native bone at the nanoscale level. Nanofiber membrane without the addition of HAp was seen as relatively smooth, well-distributed, and bead-free (Fig. 3(a)), while the morphology of nanofiber membrane PVA/PVP/CS/HAp at higher concentration of HAp shows that the agglomeration was formed at nanofiber starting HAp concentration of 1 wt% to 5 wt% (Fig. 3(b-d)). This result is confirmed by the smaller standard deviation of nanofiber without HAp than the nanofiber with higher HAp concentration, as shown in Table 2. The agglomeration occurring can be neglected because they are still in the submicron scale [20]. HAp particles are successfully incorporated and well dispersed into the fiber. The presence of HAp in fiber was expected can enhance bioactivity properties in polymer fiber because one of the drawbacks of polymeric scaffolds for biomedical applications is the lack of bioactivity properties [5]. The HAp at a concentration of 5 wt% can be incorporated into the fiber with diameter of 0.328 ± 0.049 μm (Table 2). Therefore, based on the physicochemical analysis, PVA/PVP/CS/HAp 5 wt% has the most potential to be used for bone tissue engineering to mimic ECM structure in native bone.

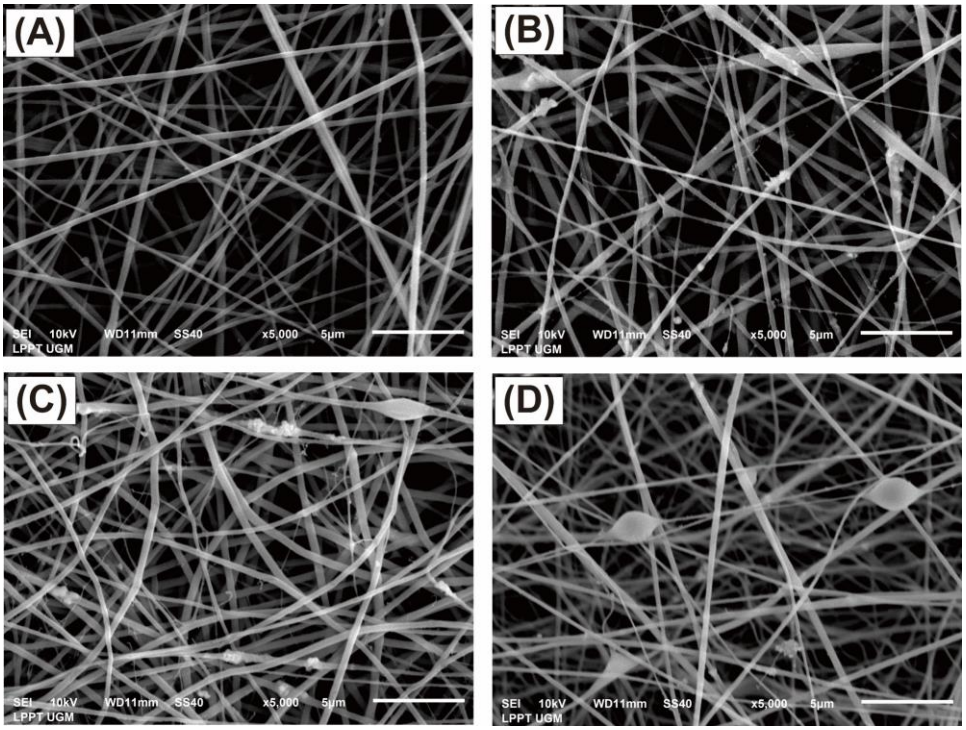

Figure 3. Morphology of nanofiber membrane PVA/PVP/CS/HAp with concentration of HAp (a) 0, (b) 1, (c) 3, (d) 5 wt%

Table 2. Diameter of nanofiber PVA/PVP/CS/HAp (a) 0, (b) 1, (c) 3, (d) 5 wt%

Sample	Diameter of Fiber (μm)
PVA/PVP/CS/HAp 0 wt%	0.357 ± 0.008
PVA/PVP/CS/HAp 1 wt%	0.463 ± 0.022
PVA/PVP/CS/HAp 3 wt%	0.397 ± 0.038
PVA/PVP/CS/HAp 5 wt%	0.328 ± 0.049

4 Conclusion

HAp derived from SL shells (*Panulirus homarus*) was successfully synthesized using precipitation methods with a hexagonal structure, and the molar ratio of Ca/P was 1.67. The XRD results showed that β-TCP was also formed, which is one of the calcium phosphates with high biocompatibility for human bones. HAp was also successfully incorporated and well dispersed into PVA/PVP/CS nanofiber membrane using the electrospinning method with small agglomerations. The addition of HAp with concentration of 1, 3, and 5 wt% as a filler into nanofiber to mimic the ECM structure of native bone at the nanoscale level and enhance the bioactivity properties of nanofiber. Based on the physicochemical analysis revealed that the nanofiber scaffold PVA/PVP/CS/HAp 5 wt% with a fiber diameter of 0.328 ± 0.049 μm has the most potential to be used for bone tissue engineering.

The authors are immensely grateful to the Ministry of Education, Culture, Research and Technology, Republic of Indonesia, Masters Education Towards Doctorate for Excellent Undergraduates Programs (PMDSU) (PT Grant 2198/UN1/DITLIT/DitLit/PT.01.03/2023) for financially supporting this research.

References

1. H. A. Permatasari and Y. Yusuf, IOP Conf. Ser.: Mater Sci Eng, **vol. 546,** no. 4, pp. 042031, (2019).
2. H. Qu, H. Fu, Z. Han, and Y. Sun, *RSC Adv.*, **vol. 9**, no. 45, pp. 26252–26262, (2019).
3. M. M. Stevens, *Materials Today*, **vol. 11**, no. 5, pp. 18–25, (2008).
4. M. Akram, R. Ahmed, I. Shakir, W. Ibrahim, and R. Hussain, *J Mater Sci*, **vol. 49**, no. 4, pp. 1461–1475, (2014).
5. R. Y. Basha, and M. Doble, *Mater Sci and Eng: C*, **vol. 57**, pp. 452–463, (2015).
6. H. D. Barth, E. A. Zimmermann, E. Schaible, S. Y. Tang, T. Alliston, and R. O. Ritchie, *Biomaterials*, **vol. 32**, no. 34, pp. 8892–8904, (2011).
7. T. Gong, J. Xie, J. Liao, T. Zhang, S. Lin, and Y. Lin, *Bone Res*, **vol. 3**, no. 1, pp. 15029, (2015).
8. S. Rujitanapanich, P. Kumpapan, and P. Wanjanoi, *Energy Procedia*, **vol. 56**, pp. 112–117, (2014).
9. S. V. Dorozhkin, *Ceramics International*, **vol. 41**, no. 10, pp. 13913–13966, (2015).
10. S. Lala, S. Brahmachari, K. Das, D. Das, T. Kar, and K. Pradhan, *Mater Sci and Eng: C*, **vol. 42**, pp. 647–656, (2014).
11. Aminatun, *Inter. J. of Poly. Mater. and Poly. Biomat.*, **vol. 72**, no. 5, pp. 376–385, (2023)
12. Y. Rizkayanti and Y. Yusuf, *Int. J. Nanoelectronic Mater*., **vol. 12**, no. 1, pp. 85-92, 2019.
13. G. Ma and X. Y. Liu, *Crystal Growth & Design*, **vol. 9**, no. 7, pp. 2991–2994, (2009).
14. R.Rial, M.G. Durruthy, Z.Liu, and J.M. Ruso, *Molecules*, **vol. 26**, no. 11, pp. 3190, (2021).
15. X. Wang, B. Ding, and B. Li, *Materials Today*, **vol. 16**, no. 6, pp. 229–241, (2013).
16. M. Tahir, S. Vicini, and A. Sionkowska, *Polymers*, **vol. 15**, no. 7, pp. 1654, (2023).
17. S. Wu, K. Li, W. Shi, and J. Cai, *Inter. J. Biological Macro*, **vol. 210**, pp. 76–84, (2022).
18. P. Franco and I. De Marco, *Polymers*, **vol. 12**, no. 5, pp. 1114, (2020).
19. K. Desai, K. Kit, J. Li, and S. Zivanovic, *Bio.*, **vol. 9**, no. (3), pp. 1000-1006, (2008).
20. I. K. Januariyasa, I. D. Ana, and Y. Yusuf, *Mater. Sci. and Eng.: C*, **vol. 107**, pp. 110347, (2020).
21. IK.H. Dinatha, A. Jamilludin, I. Supii, H. Wihadmadyatami, J. Partini, Y. Yusuf, *Material Science Forum*; **vol. 1090**, pp 39–44, (2023).
22. M. Sari, P. Hening, Chotimah, I. D. Ana, and Y. Yusuf, *Biomater Res*, **vol. 25**, no.1,pp. 2, (2021).
23. D. Patty, A. Nugraheni, D. Ana, and Y. Yusuf, *JBMR B*, **vol. 110**, no. 6, pp. 1412–1424, (2022).
24. V. J. Mawuntu and Y. Yusuf, *J. Asi Cer. Soc.*, **vol. 7**, no. 2, pp. 161-169, (2019).
25. W. Ho, H. Hsu, S. Hsu, W. Hung, and C. Wu, *C. Inter.*, **vol. 39**, no. 6, pp. 6467–6473, (2013).
26. S. Wu, K. Li, W. Shi, and J. Cai, *Carb. Polymers*, **vol. 294**, pp. 119756, (2022).
27. C. Christou, K. Philippou, K. Christoforou, and I. Pas, *Carbo Poly*, **vol. 219**, pp. 298–305, (2019).
28. T. Jia, J. Gong, H. Gu, Y. Kim, J. Dong, and Y. Shen, *Carbo Poly*, **vol. 67**, pp. 403–409, (2007).